PHYSICAL REVIEW B VOLUME 49, NUMBER 9 1 MARCH 1994-I

Influence of hole filling by Hf and hole doping by Ca on the superconductivity and flux pinning of $YBa_2Cu_3O_{7-\delta}$

R. G. Kulkarni,* I. A. Shaikh, J. A. Bhalodia, G. J. Baldha, and D. G. Kuberkar
Department of Physics, Saurashtra University, Rajkot-360 005, India

(Received 3 May 1993; revised manuscript received 18 October 1993)

The structural and superconducting properties of $(Y_{1-x-y}Ca_yHf_x)Ba_2Cu_3O_z$ samples are investigated using resistivity, ac susceptibility, and dc magnetization measurements. The effect of increasing the Hf concentration in $Y_{1-x}Hf_xBa_2Cu_3O_z$ lowers the oxygen content and decreases T_c. The substitution of Ca for Y in $(Y_{0.85-y}Ca_yHf_{0.15})Ba_2Cu_3O_z$ provides proper matching between the ionic radius and valence of Y^{3+} (0.89 Å) and the average ionic radius and valence of Hf^{4+} (0.78 Å) and Ca^{2+} (0.99 Å). As the Ca content increases, the T_c increases from $y=0$ (74 K) to $y=0.15-0.20$ (compensated oxides) having T_c of 84.5–85.5 K. Magnetization measurements on powdered Hf-doped samples exhibit pronounced $M(H)$ hysteresis loops indicative of extensive flux pinning and enhanced critical currents.

I. INTRODUCTION

The superconducting transition temperature T_c of $YBa_2Cu_3O_{7-\delta}$ (YBCO) materials depends on the mobile carrier concentration p or the effective copper valence in the Cu-O_2 plane. The oxygen content controls p in a nonlinear fashion[1,2] because carriers are distributed in both the planes and the Cu-O chains. In addition to varying the oxygen content, cation doping,[3–10] e.g., at the Y site, may also change p and affect many properties accordingly.

Among all cation dopings, Pr substitution for Y in $Y_{1-x}Pr_xBa_2Cu_3O_{7-\delta}$ (YPrBCO) has been extensively examined by numerous workers. Recently, Radousky[3] has reviewed in great detail the superconducting, structural, magnetic, and other properties of $Y_{1-x}Pr_xCu_3O_{7-\delta}$ and lists 156 references. It has also been shown that the suppression of T_c by Pr substitution in YBCO can be compensated by appropriate hole doping with Ca to some extent.[4,5]

The valence state of Ca^{2+} is lower than that of Y^{3+}; such a substitution will increase p due to hole doping by Ca. The effect of Ca doping in pure YBCO has been studied extensively.[5–10] The valence state of Hf^{4+} is higher than that of Y^{3+} and the ionic radius of Hf^{4+} (0.78 Å) is about 0.1 Å smaller than that of Y^{3+} (0.89 Å); a substitution with Hf may decrease p due to hole filling by Hf. The average ionic radius and valence of Ca^{2+} (0.99 Å) and Hf^{4+} (0.78 Å) in equal proportions match those of Y^{3+} (0.89 Å); a substitution with Hf and Ca will lead to a compensated oxide having T_c closer to that of pure YBCO. Therefore it is of interest to investigate the effect of Hf substitution for Y in YBCO on superconductivity, oxygen content, and flux pinning. In order to understand the behavior of Hf with respect to the YBCO structure, the simultaneous substitution of Hf and Ca at the Y site has been undertaken.

In this paper, we report x-ray diffraction, resistivity, ac susceptibility, and dc magnetization measurements on the series of compounds having the stoichiometric compositions $Y_{1-x}Hf_xBa_2Cu_3O_z$ (YHfBCO) for $x=0.0-0.2$ and $(Y_{1-x-y}Ca_yHf_x)Ba_2Cu_3O_z$ (YHfCaBCO) for $x=0.15$ and $y=0.0-0.40$. The interrelationship between the superconducting transition temperature and the variation of the oxygen content is discussed in the context of the effective copper valence.

II. EXPERIMENT

A series of compounds having the compositions $Y_{1-x}Hf_xCu_3O_z$ ($x=0.0,0.05,0.10,0.15,0.20$) and $Y_{1-x-y}Ca_yHf_xBa_2Cu_3O_z$ ($x=0.15, y=0.05,0.10,0.15,0.20,0.30,0.40$) were synthesized by a standard ceramic technique[11] under identical conditions. Stoichiometric quantities of fine powders of Y_2O_3, $BaCO_3$, CuO, HfO_2, and CaO (all 99.9% pure) were thoroughly mixed and heated in air at 950 °C for 24 h in a platinum crucible. This reacted powder was reground and reheated at 950 °C for 24 h to obtain a homogeneous single-phase sample. The black product was then pulverized and cold-pressed into pellets which were sintered in air at 950 °C for 24 h. To obtain fully oxygenated samples, these pellets were annealed under oxygen flow at 450 °C for 12 h followed by slow cooling at the rate of $1\,°C\,min^{-1}$ until room temperature was reached.

All the samples were characterized at room temperature by x-ray diffraction using Cu $K\alpha$ radiation. The x-ray analysis revealed that all the samples were single phase, with an impurity level of less than 1%. The stoichiometric composition of the constituents in the sample was confirmed by energy-dispersive x-ray analysis using a JEOL scanning electron microscope. The oxygen content was determined by the iodometric method. Resistivity was measured as a function of temperature on regularly shaped samples using the standard four-probe method. The ac susceptibility was measured by an inductive technique with a frequency of 313 Hz at 50 mV. dc magnetization measurements were performed using an EG&G PAR model 4500 vibrating-sample magnetometer (VSM) with a 10-kOe electromagnet. An APD closed-

0163-1829/94/49(9)/6299(6)/$06.00

cycle-refrigerator cryostat was used to cool the sample in the temperature range $12 < T < 100$ K.

III. RESULTS AND DISCUSSION

An excellent agreement amongst x-ray-diffraction patterns of YHfBCO, YHfCaBCO, and YBCO is an indication that the compounds YHfBCO and YHfCaBCO have the YBCO structure. The observed x-ray-diffraction peaks were modeled by modified Gaussian functions and the refined unit-cell parameters, calculated using a standard least-squares program, are listed in Table I. All four Hf-doped samples ($x = 0.05-0.20$) and four of the Hf-Ca-doped samples ($x = 0.15$, $y = 0.05-0.20$) remain orthorhombic with distortion $(b-a)/(b+a)$ very close to that of pure YBCO, while two Hf-Ca-doped samples ($x = 0.15, y = 0.3, 0.4$) approach towards tetragonal.

Table I shows the behavior of the lattice parameters a, b, and c as a function of x and y. The lattice parameters of $Y_{1-x}Hf_xBa_2Cu_3O_z$ for $x = 0.0, 0.05, 0.10$ display oscillating behavior in a and c, while for the $x = 0.15$ and 0.20 concentrations all three lattice parameters exhibit constant values. The observed peculiar behavior of the lattice parameters of Hf-doped samples indicates that either Hf may not be entering the YBCO structure uniformly as the nominal concentration of Hf is increased, or the smaller ionic radius of Hf^{4+} (0.78 Å) compared to Y^{3+} (0.89 Å) may not cause noticeable structural effects similar to the ones observed with Pr^{3+} (0.98 Å).[3] However, there is an overall volume increase from 173.34 to 174.54 Å^3 for Hf-doped samples with $x = 0.0-0.2$, which is consistent with the observed volume increase from 173.57 to 174.66 Å^3 for Pr-doped samples with $x = 0.0-0.2$.[3] In the Ca-doped series, the lattice parameters are approximately constant until $y = 0.3$, with nearly constant volume, which is consistent with the simple picture of an average ionic radius of Hf^{4+} (0.78 Å) and Ca^{2+} (0.99 Å) matching Y^{3+} (0.89 Å). A sharp jump for $y > 0.3$ occurs due to a structural transition from orthorhombic to tetragonal at $y = 0.4$. These structural considerations indicate that the nominal concentrations are close to the actual concentrations in the samples.

Oxygen content of the single-phase Hf- and Hf-Ca-doped YBCO samples was determined by an iodometric titration technique. The values are listed in Table I. The effective Cu valence $(2+p)$ or the hole concentration (p) per [Cu-O] unit was calculated from these data and is included in the table. p and z denote the hole concentration per [Cu-O] unit and the oxygen content, respectively. The substitution of Hf^{4+} in place of Y^{3+} is quite different from Hf^{4+} substitution in place of either Ba^{2+} or Cu^{2+}. Such a substitution in place of Y leads to a decrease in the effective copper valence compared to the pure YBCO, whereas substitution in place of Ba or Cu increases the oxygen content essentially in the Cu-O chain regions.[12-14] It is evident from Table I that both p and z decrease with increasing Hf content in $Y_{1-x}Hf_xBa_2Cu_3O_z$ for $x = 0.0-0.2$, indicating that Hf^{4+} replaces Y^{3+}, while both p and z increase with increasing Ca concentration in $(Y_{0.85-y}Ca_yHf_{0.15})Ba_2Cu_3O_z$ for $y = 0.0-0.4$, demonstrating that Ca^{2+} replaces Y^{3+}.

Typical resistivity results from our Hf- and Hf-Ca-doped samples are displayed in Figs. 1(a) and 1(b). Table II shows the resistive superconducting transition temperatures: onset, midpoint, and zero resistance. The Hf ions suppress the superconductivity very effectively at an average rate of ~1 K per at. % of Hf. The suppression in $T_c^{\mathrm{mid}}(R)$ by Hf substitution is compensated by the addition of holes by Ca doping at constant Hf concentration. This is shown by observing the increase in T_c with increasing y for $(Y_{0.85-y}Ca_yHf_{0.15})Ba_2Cu_3O_z$. The temperature dependence of the ac susceptibility χ_{ac} for $y = 0.05-0.2$ in $(Y_{0.85-y}Ca_yHf_{0.15})Ba_2Cu_3O_z$ is shown in Fig. 2, and the onset critical temperature determined from ac susceptibility, $T_c(\chi_{\mathrm{ac}})$, is listed in Table II. Pellets of YHfBCO and YHfCaBCO were finely crushed to powder and the average particle diameter was measured (using differential-interference contrast optical microscopy) to be about 1×10^{-3} cm. The powdered samples were cooled in zero external field during recording of the dc

TABLE I. Lattice parameters, orthorhombicity, oxygen content, and effective Cu valence of $(Y_{1-x-y}Hf_xCa_y)Ba_2Cu_3O_2$.

Sample	Lattice parameters (Å)			Orthorhombicity	Oxygen content	Cu valence
(x,y)	a	b	c	$10^2\left[\frac{b-a}{b+a}\right]$	z	$2+p$
(0.0,0.0)	3.8217(5)	3.8875(5)	11.6672(11)	0.853	6.83(3)	2.220
(0.05,0.0)	3.8198(5)	3.8841(5)	11.6475(11)	0.834	6.82(3)	2.197
(0.10,0.0)	3.8261(5)	3.8885(5)	11.6690(11)	0.804	6.80(3)	2.167
(0.15,0.0)	3.8400(5)	3.8897(5)	11.6893(11)	0.643	6.70(3)	2.083
(0.20,0.0)	3.8398(5)	3.8893(5)	11.6876(11)	0.640	6.65(3)	2.033
(0.15,0.05)	3.8396(5)	3.8886(5)	11.6883(11)	0.634	6.73(3)	2.120
(0.15,0.10)	3.8410(5)	3.8892(5)	11.6887(11)	0.623	6.84(3)	2.210
(0.15,0.15)	3.8408(5)	3.8887(5)	11.6880(11)	0.620	6.96(3)	2.307
(0.15,0.20)	3.8395(5)	3.8886(5)	11.6886(11)	0.635	7.03(3)	2.370
(0.15,0.30)	3.8450(5)	3.8600(5)	11.6872(11)	0.195	7.07(3)	2.460
(0.15,0.40)	3.8453(5)	3.8467(5)	11.6878(11)	0.018	7.12(3)	2.500

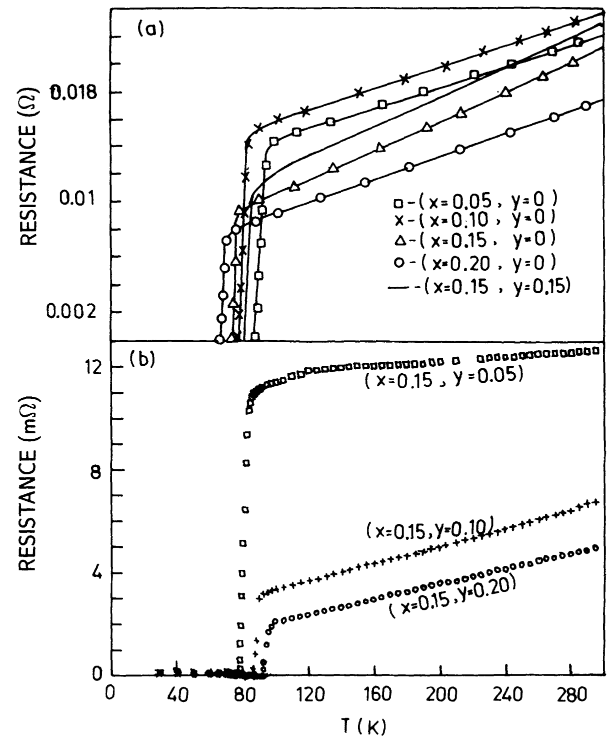

FIG. 1. Resistance vs temperature for $(Y_{1-x-y}Hf_xCa_y)Ba_2Cu_3O_z$. (a) $(x=0.05, y=0), (x=0.10, y=0), (x=0.15, y=0), (x=0.20, y=0)$, and $(x=0.15, y=0.15)$. (b) $(x=0.15, y=0.05), (x=0.15, y=0.10)$, and $(x=0.15, y=0.20)$.

magnetization curves at several temperatures in the range $12 < T < 100$ K. Figure 3 shows typical magnetization $M(H)$ scans obtained at $T=13$ and 40 K for samples with $x=0.1$ and 0.2, respectively, exhibiting pronounced $M(H)$ hysteresis loops indicative of large flux pinning. The magnetic susceptibility determined as a function of temperature from the magnetization results is shown in Fig. 4 for typical samples, and the magnetic onset transition temperatures $T_c(\chi_{\text{mag}})$ are listed in Table II. It is evident from Table II that $T_c^{\text{mid}}(R)$, $T_c(\chi_{\text{ac}})$, and $T_c(\chi_{\text{mag}})$ agree very well with each other. This shows the consistency of the measurements and the high quality of the samples.

We have shown in Fig. 5 (a) T_c versus Hf concentration x and in Fig. 5(b) T_c versus Ca concentration y for one Hf concentration $(x=0.15)$. For the sake of comparison and completeness, we have also shown in Fig. 5(a) the reduction of T_c with Pr concentration x in $(Y_{1-x}Pr_x)Ba_2Cu_3O_{6.95}$ and in Fig. 5(b) the variation of T_c with Ca concentration y in $(Y_{0.85-y}Ca_yPr_{0.15})Ba_2Cu_3O_{6.95}$. The data for both systems was taken from Refs. 3 and 4.

It is evident from Fig. 5(a) that there is a disagreement between the suppression of T_c with Hf and Pr concentrations of YHfBCO and YPrBCO,[4] respectively. This disagreement suggests that the valence of Pr is not +3.90 as claimed,[4] but is closer to the accepted value of +3.10.[3]

The observed suppression of T_c by Hf substitution in YBCO is explained on the basis of the oxygen effect assuming it is real. The oxygen content z of a superconductor is directly related to the hole concentration p or the effective Cu valence $2+p$, which controls the superconductivity. The concentration of holes can be varied by varying the Hf doping concentration. It is evident from Table I that T_c decreases from 92 to 67 K as z decreases from 6.83 to 6.65 with corresponding increase of x from 0.0 to 0.2. The trend is clear: the hole concentration p decreases as the samples are doped with higher concentrations of Hf^{4+} for Y^{3+}. The additional electrons contributed by Hf ions are expected to fill mobile holes in the CuO_2 planes, reducing conduction and eliminating superconductivity. As a matter of fact, p decreases from 0.220 to 0.033 as x increases from 0.0 to 0.2, with a corresponding decrease in T_c from 92 to 67 K (Table I). Our results agree with the T_c-oxygen-content behavior observed in orthorhombic YBCO, in which T_c decreases with decreasing oxygen content from 6.85 to 6.50.[15] These re-

TABLE II. T_c values obtained from measurements of resistivity, ac susceptibility, and dc magnetization for $(Y_{1-x-y}Hf_xCa_y)Ba_2Cu_3O_z$. All T_c values in K.

Sample		Resistivity		ac susceptibility	dc magnetization
(x,y)	T_c^{on}	T_c^{mid}	$T_c^{R=0}$	$T_c(\chi_{\text{ac}})$	$T_c(\chi_{\text{mag}})$
(0.0,0.0)	93.0(1)	92.0(1)	91.0(1)	91.5(1)	92.0(1)
(0.05,0.0)	88.7(1)	87.5(1)	86.5(1)		
(0.10,0.0)	84.5(1)	81.5(1)	79.0(1)		80.0(1)
(0.15,0.0)	77.5(1)	74.0(1)	72.0(1)		
(0.20,0.0)	71.0(1)	67.0(1)	65.0(1)		67.0(1)
(0.15,0.05)	81.5(1)	78.5(1)	76.0(1)	76.0(1)	
(0.15,0.10)	82.5(1)	80.5(1)	78.5(1)	79.0(1)	80.0(1)
(0.15,0.15)	86.5(1)	84.5(1)	82.2(1)	84.5(1)	
(0.15,0.20)	89.0(1)	85.5(1)	82.8(1)	85.0(1)	85.0(1)
(0.15,0.30)	82.5(1)	80.5(1)	79.0(1)		
(0.15,0.40)	83.0(1)	78.0(1)	72.0(1)		78.0(1)

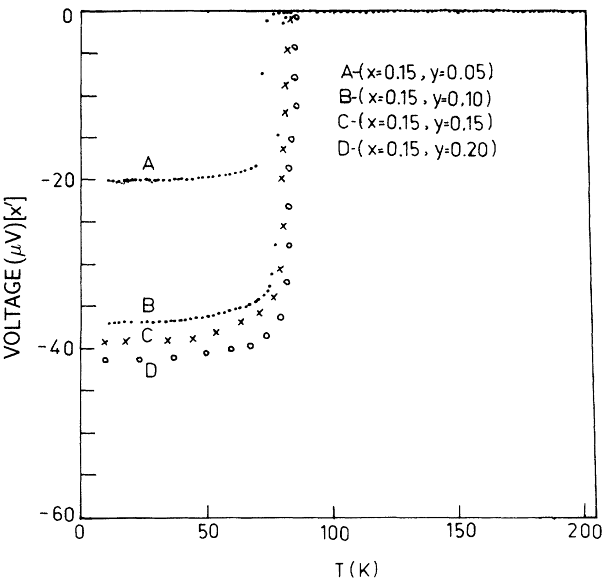

FIG. 2. Temperature dependence of ac susceptibility for $(Y_{0.85-y}Ca_yHf_{0.15})Ba_2Cu_3O_z$ for $y = 0.05$, 0.10, 0.15, and 0.20.

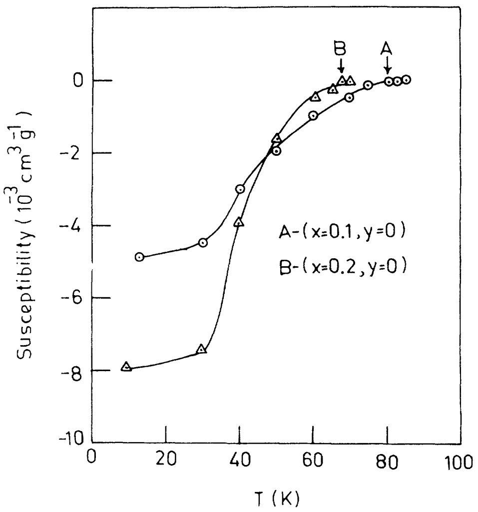

FIG. 4. Magnetic susceptibility as a function of temperature for $(Y_{1-x}Hf_x)Ba_2Cu_3O_z$.

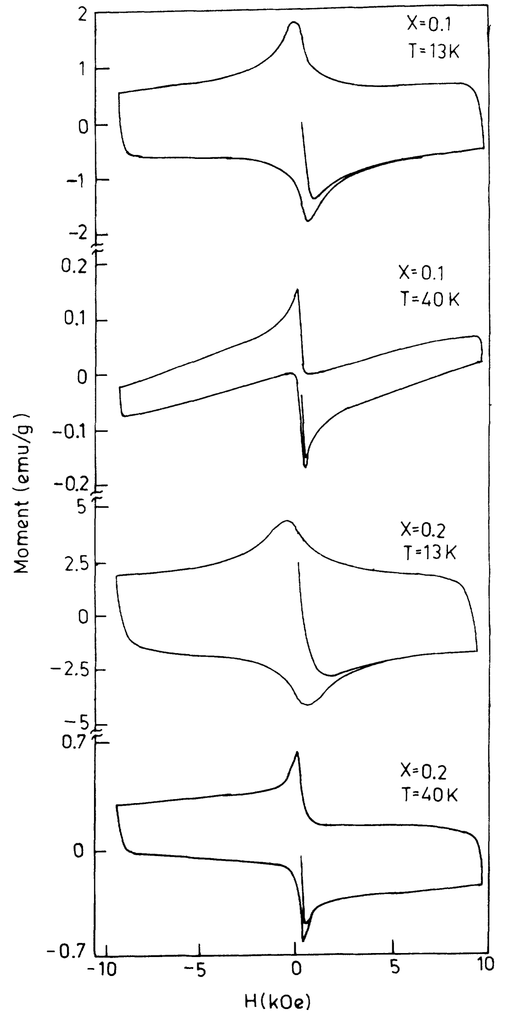

FIG. 3. Magnetic hysteresis loops for $(Y_{1-x}Hf_x)Ba_2Cu_3O_z$ with $x = 0.1$ and 0.2 at $T = 13$ and 40 K.

sults clearly establish that the effect of increasing Hf content in YHfBCO is equivalent to that of decreasing oxygen content in YBCO.

It is evident from Fig. 5(b) that the T_c of $(Y_{0.85-y}Ca_yHf_{0.15})Ba_2Cu_3O_z$ increases with increasing y up to $y = 0.2$, exhibiting a maximum at $y = 0.2$ ($T_c^{\max} \sim 85.5$ K), and thereafter it decreases with further increase in y for $0.2 < y < 0.4$. This implies that the reduction in T_c from 92 K ($x = 0.0$) to 74 K ($x = 0.15$) is compensated by the addition of holes by 5–20 at. % Ca ($y = 0.05$–0.20). This counteracts hole filling and increases T_c from 74 to 85.5 K nearly linearly with y. Such a behavior has indeed been observed and displayed in Fig. 5(b). A noteworthy fact is that the T_c-vs-y data shown in Fig. 5(b) for $(Y_{0.85-y}Ca_yPr_{0.15})Ba_2Cu_3O_{6.95}$ (Ref. 4) should have displayed compensation at $y = 0.15$ (T_c maximum) if the valence of Pr was +4. On the contrary, the data show lowest T_c at $y = 0.15$, indicating that the valence of Pr in this system is not +4, but +3.10, the accepted value,[3] consistent with the maximum at $y = 0.02$ shown in Fig. 5(b).

The dependence of T_c on Ca concentration in $(Y_{0.85-y}Ca_yHf_{0.15})Ba_2Cu_3O_z$ [Fig. 5(b)] is explained as follows. Both oxygen content and hole concentration increase as the samples are doped with higher concentrations of Ca, as shown in Table I. The T_c of $(Y_{0.85-y}Ca_yHf_{0.15})Ba_2Cu_3O_z$ increases with increasing y as p increases up to the optimum value 0.37 ($y = 0.2, T_c^{\max} = 85.5$ K). The oxides around the optimum value of p are identified as compensated oxides, with $x = 0.15$ at $y = 0.15$ and 0.20, displaying T_c's of 84.5 and 85.5 K, respectively. The T_c's of these oxides lie closer to that of pure YBCO ($T_c = 92$ K), as expected from ionic-radius and valence considerations. Moreover, in these compensated oxides, the hole filling by Hf is completely balanced by hole doping from Ca. For further increase of

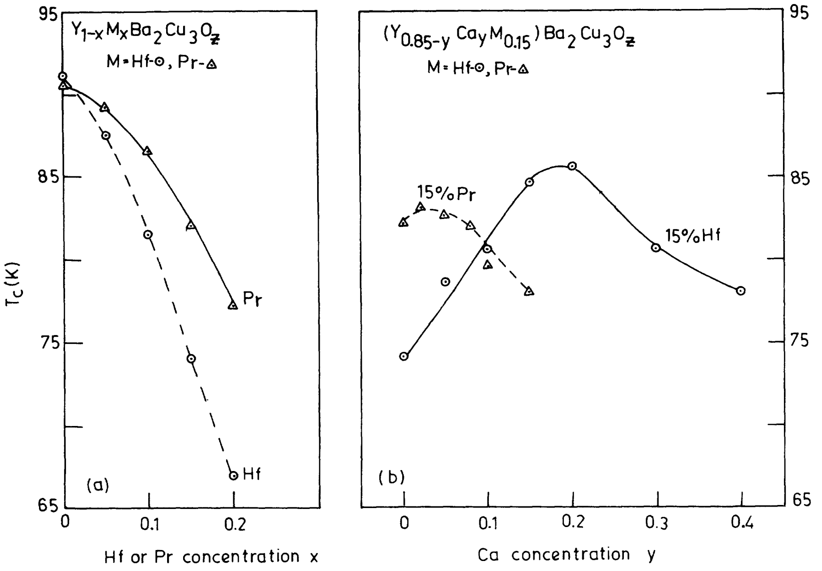

FIG. 5. (a) T_c versus Hf and Pr concentration x in $(Y_{1-x}M_x)Ba_2Cu_3O_z$ with M =Hf or Pr. Pr values from Ref. 3. (b) T_c versus Ca concentration y for $x=0.15$ in $(Y_{0.85-y}Ca_yM_{0.15})Ba_2Cu_3O_z$ with M=Hf or Pr. Pr values from Ref. 4.

p from 0.37 to 0.50 ($y=0.2$–0.4), T_c decreases from 85.5 to 78 K due to excess hole doping by Ca. As a matter of fact, excess holes doped by Ca in samples with $x=0.15$ at $y=0.30$ and 0.40 not only reduce T_c but also induce a structural transformation from orthorhombic to tetragonal (see lattice parameters, Table I). Similar behavior (reduction in T_c) due to hole over-doping has been observed in $YBa_2Cu_3O_7$ (Refs. 15 and 16) and $LaBa_2Cu_3O_{7-\delta}$.[17]

It is customary to use magnetization measurements as a contactless method for determining the intragrain critical current density J_c. From the width of the hysteresis loop, it is possible to estimate J_c in the superconducting portions of the samples using the Bean critical-state model.[18] For a spherical grain of radius R in cm, J_c in A cm^{-2} can be expressed in terms of the magnetization M in emu cm^{-3} to a first approximation by the relation,[19]

$$J_c=\frac{15[M^+-M^-]}{R}, \tag{1}$$

where M^+ and M^- are the moments observed while sweeping the magnetic field up and down, respectively. Using $R=5\times10^{-4}$ cm, $\rho=5$ g cm^{-3} (measured density) and Eq. (1), values of $J_c(H)$ at different temperatures have been calculated for YHfBCO at $x=0.1$ and 0.2, and the results are displayed in Fig. 6. It is evident from Fig. 6 that J_c decreases with increasing temperature T, while it remains nearly constant with applied magnetic field H between 2 and 9 kOe. For the sake of comparison, we have also shown in Fig. 6 our data for J_c versus H in a pure YBCO sample ($x=0.0$) at $T=12$ K. Our J_c value for the $x=0.0$ sample at $T=12$ K and $H=8$ kOe is $\sim10^5$ A cm^{-2} and is in very good agreement with the J_c obtained by flux-profile measurements[20] on a pure YBCO polycrystalline sample, which was estimated to be $\sim10^5$ A cm^{-2} at $T=13$ K and $H=8$ kOe. It is evident from Fig. 6 that, the J_c values for Hf-doped samples, with $x=0.1$ and 0.2 are, respectively, 2.0 and 5.5 times larger than the J_c value of the pure YBCO sample at $T=12$ K and $H=8$ kOe. This indicates that the Hf substitution for Y does enhance flux pinning in YBCO and that dopants act as pinning centers. The flux-creep model is not applicable to our data.

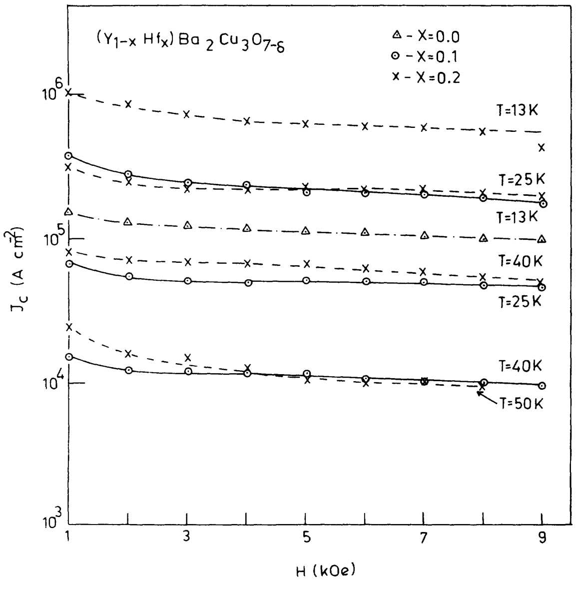

FIG. 6. Magnetic-field dependence of J_c for the Hf-doped YBCO samples at various temperatures.

In conclusion, the observed lowering of T_c with increasing x in $Y_{1-x}Hf_xBa_2Cu_3O_z$ provides convincing evidence that the filling of holes by Hf^{4+} reduces the hole concentration and suppresses superconductivity. This suppression can be compensated by appropriate hole doping with Ca. This has been shown by the fact that Ca doping in $(Y_{0.85-y}Ca_yHf_{0.15})Ba_2Cu_3O_z$ with $y = 0.0-0.2$ increases T_c from 74 ($y = 0.0$) to 85.5 K ($y = 0.2$), closer to the value of 92 K for pure YBCO ($x = y = 0$). By comparison of critical currents and flux pinning between pure YBCO and Hf-doped YBCO, it is found that Y-site doping increases J_c in the YBCO system.

ACKNOWLEDGMENTS

The authors are thankful to Professor P. Boolchand, University of Cincinnati, for providing VSM facilities. This research project was financially supported by the Department of Atomic Energy, India.

---

*Author to whom all correspondence should be addressed.

[1] R. J. Cava, A. W. Hewat, E. A. Hewat, B. Batlogg, M. Marczio, K. M. Rabe, J. J. Krajewski, W. F. Peck, Jr., and L. W. Rupp, Jr., Physica C **165**, 419 (1990).

[2] Y. Tokura, J. B. Torrance, T. C. Huang, and A. I. Nazzal, Phys. Rev. B **38**, 7156 (1988).

[3] H. B. Radousky, J. Mater. Res. **7**, 1917 (1992), and references therein.

[4] J. J. Neumeier, T. Bjornholm, M. B. Maple, and I. K. Schuller, Phys. Rev. Lett. **63**, 2516 (1989).

[5] G. K. Bichile, Smita Deshmukh, D. G. Kuberkar, and R. G. Kulkarni, Physica C **183**, 154 (1991).

[6] M. W. Shafer, T. Penny, and B. L. Olson, Phys. Rev. B **36**, 4047 (1987).

[7] R. G. Kuckley, D. M. Pooke, J. L. Tallon, M. R. Presland, N. E. Flower, M. P. Staines, H. L. Johnson, M. Meylan, G. V. M. Williams, and M. Bowden, Physica C **174**, 383 (1991).

[8] A. Manthiram and J. B. Goodenough, Physica C **159**, 760 (1989).

[9] E. Suarad, A. Maignan, V. Cainaert, and B. Raveau, Physica C **200**, 43 (1992).

[10] Y. Sun, G. Strasser, E. Gornik, W. Scidenbusch, and W. Rauch, Physica C **206**, 291 (1993).

[11] R. G. Kulkarni, G. J. Baldha, G. K. Bichile, D. G. Kuberkar, and S. Deshmukh, Appl. Phys. Lett. **59**, 1386 (1991).

[12] K. Kinoshita, A. Matsuda, H. Shibata, T. Ishii, T. Watanabe, and T. Yamada, Jpn. J. Appl. Phys. **27**, L1642 (1988).

[13] S. Li, E. A. Hayri, K. V. Ramanujachary, and M. Greenblatt, Phys. Rev. B **38**, 2450 (1988).

[14] P. F. Miceli, J. M. Tarascon, L. H. Greene, P. Barboux, F. J. Rotella, and J. D. Jorgensen, Phys. Rev. B **37**, 5932 (1988).

[15] W. R. McKinnon, M. L. Post, L. S. Selwyn, G. Pleizier, J. M. Tarascon, P. Barboux, L. H. Greene, and G. W. Hull, Phys. Rev. B **38**, 6543 (1988).

[16] M. Ohkubo and T. Hioki, Solid State Commun. **79**, 255 (1991).

[17] Yi Song, J. P. Golben, X. D. Chen, J. R. Gaines, M. S. Wong, and E. R. Kreidler, Phys. Rev. B **38**, 2858 (1988).

[18] C. P. Bean, Rev. Mod. Phys. **36**, 31 (1964).

[19] J. O. Willis, J. R. Cost, R. D. Brown, J. D. Thompson, and D. E. Peterson, IEEE Trans. Magn. **25**, 21 (1989).

[20] H. Kupfer, I. Apfelstedt, R. Flkiger, C. Keller, R. Meier-Hirmer, B. Runtsch, A. Turowsk, U. Wiech, and T. Wolf, Cryogenics **29**, 268 (1989).